Using the Non-Intrusive Load Monitor for Shipboard Supervisory Control

Robert W. Cox, *Member, IEEE*, LCDR Patrick L. Bennett, LCDR T. Duncan McKay, James Paris, Steven B. Leeb, *Fellow, IEEE*

***Abstract*— Field studies have demonstrated that it is possible to evaluate the state of many shipboard systems by analyzing the power drawn by electromechanical actuators [1], [2], [3], [4], [5]. One device that can perform such an analysis is the non-intrusive load monitor (NILM). This paper investigates the use of the NILM as a supervisory control system in the engineering plant of gas-turbine-powered vessel. Field tests conducted at the Navy's DDG-51 Land-Based Engineering Site (LBES) demonstrate that the NILM can potentially reduce overall sensor count if used in a supervisory control system.**

I. Introduction

ENGINEERING plants in modern naval vessels consist of complex networks of electrical and mechanical actuators. In many cases, high-level supervisory systems are required to control the interactions between these devices. To ease maintenance operations, new supervisory systems are also designed to assist in condition-based maintenance. For example, high-level controllers for many gas turbines can now record sensor data and, in some cases, they can even perform automated data assessment [7]. Because of the potential cost savings, there is a push to extend the capabilities of such systems [8], [9]. Doing so, however, usually means that more sensors are deployed throughout the engineering plant. In fact, some estimates indicate that each vessel in the new DDG-1000 class will feature as many as 200,000 sensing devices [10]. Although such a large sensing network may seem advantageous, it can also be both expensive and difficult to maintain. A simple, low-cost alternative with lower sensor density could provide identical information with higher reliability. At a minimum, such an alternative could serve as a high reliability backup for an existing sensor network

One device that can greatly simplify the supervisory monitoring and control process is the non-intrusive load monitor (NILM) [6], [11]. The NILM, which measures the current and voltage at one or more central locations in a power-distribution network, can determine both the operating schedule and the operational status of each of the major loads in an engineering plant [4], [12], [13]. In many cases the NILM can also use its electrical data to assess the status of certain mechanical elements such as air filters and components in fluid power systems [1], [2], [3]. Because a NILM-based monitor greatly reduces the number of required sensors, it can decrease costs and increase the effectiveness of organizational-level maintenance.

To demonstrate the NILM's capabilities in supervisory control systems, we are conducting experiments at the U.S. Navy's Land-Based Engineering Site (LBES) in Philadelphia. Following a description of both the LBES facility and the NILM itself, this paper presents some results obtained during our preliminary field studies. The paper also describes our on-going efforts to further demonstrate and develop the NILM's capabilities in supervisory control systems.

II. LBES Overview

The Navy's DDG-51 LBES is designed to replicate the Number Two Main Engine Room aboard one of the Navy's *Arleigh Burke* (DDG-51) class destroyers. The equipment installed in this facility includes two LM2500 gas-turbine propulsion main engines (GTMs); three gas-turbine generators (GTGs); and auxiliary systems providing fuel oil, lube oil, low-pressure air, and cooling water. Additionally, the main engines drive a full-scale propulsion train complete with main reduction gear, shafting, and bearings [6]. A perspective view of this facility is shown in Fig. 1.

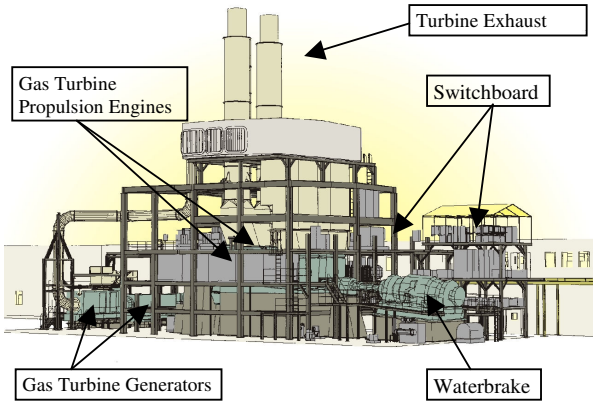

Fig. 1. Perspective view of the DDG-51 LBES.

This work was supported in part by the Grainger Foundation, the United States Coast Guard, the U. S. Navy through ONR's ESRDC program, and NAVSEA.

R. W. Cox is with the University of North Carolina-Charlotte, Charlotte, NC, 28223 USA (e-mail: rcox3@uncc.edu).

P. L. Bennett is with the United States Navy and also with the Massachusetts Institute of Technology, Cambridge, MA, 02139 USA (e-mail: bennettp@mit.edu).

T. D. McKay is with the United States Navy (e-mail: duncan.mckay@alum.mit.edu).

J. Paris and S. B. Leeb are with the Massachusetts Institute of Technology, Cambridge, MA, 02139 USA (e-mail: {bigjim,sbleeb}@mit.edu).

There are some significant differences between the land-based facility and the machinery spaces on the DDG-51. First, the LBES has a full Zonal Electrical Distribution System (ZEDS), which represents the entire shipboard electric plant of a DDG-51. Thus, the LBES features all three of the Ship's Service Gas Turbine Generators (GTGs). In reality the Number Two Main Engine Room on the DDG-51 houses only one GTG. Additionally, the ZEDS at LBES is physically collocated with the propulsion plant, but it does not supply power to the plant's auxiliary systems. At the LBES the ZEDS supplies several large load banks, and power for auxiliary systems is provided by the regional utility. A third critical difference is that the LBES does not have a propeller. In order to simulate the resistance of the ocean on the propulsion train, a large water brake is installed at the end of a shortened shaft [6].

III. NILM Overview

Figure 2 shows the block diagram of a standard NILM. Note that the NILM measures the aggregate current flowing to a bank of electrical loads. It then disaggregates the operating schedule of individual loads using signal-processing techniques. In an engineering plant, the candidate installation locations include generator output busses and distribution panels.

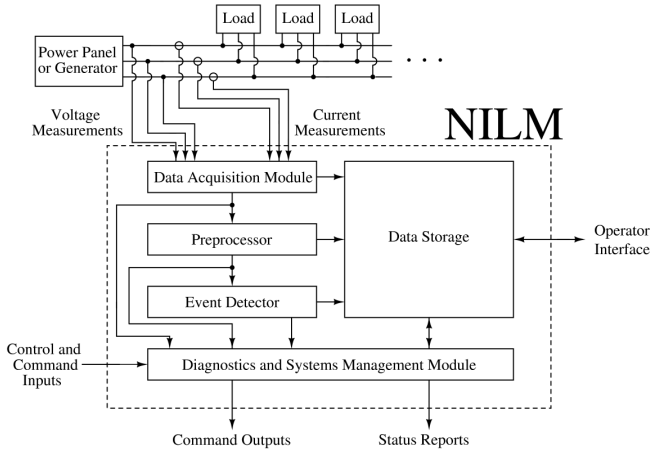

Fig. 2. Diagram showing the fundamental signal flow path in a NILM.

Using measurements of the line voltage and aggregate current, a software-based preprocessor onboard the NILM computes time-varying estimates of the frequency content of the measured line current [13]. Formally, these time-varying estimates, or spectral envelopes, are defined as the quantities [14]

$$a_m(t) = \frac{2}{T}\int_{t-T}^{t} i(\tau)\sin(m\omega\tau)\,d\tau \qquad (1)$$

and

$$b_m(t) = \frac{2}{T}\int_{t-T}^{t} i(\tau)\cos(m\omega\tau)\,d\tau\,. \qquad (2)$$

These equations are Fourier-series analysis equations evaluated over a moving window of length T [15]. The coefficients $a_m(t)$ and $b_m(t)$ contain time-local information about the frequency content of $i(t)$. Provided that the basis terms $\sin(m\omega t)$ and $\cos(m\omega t)$ are synchronized to the line voltage, the spectral envelope coefficients have a useful physical interpretation as real, reactive, and harmonic power [12], [14].

The spectral envelopes computed by the preprocessor are passed to an event detector that identifies the operation of each of the major loads on the monitored electrical service. In a modern NILM, identification is performed using both transient and steady-state information [16]. Field studies have demonstrated that transient details are particularly powerful because the transient electrical behavior of a particular load is strongly influenced by the physical task that is performed [12]. As shown in Fig. 3, for example, the physical differences between an incandescent lamp and an induction machine result in vastly different transient patterns. Figure 4 demonstrates the positive identification of an induction motor driving a small vacuum pump. Further details of the detection and identification process can be found in [16] and [17].

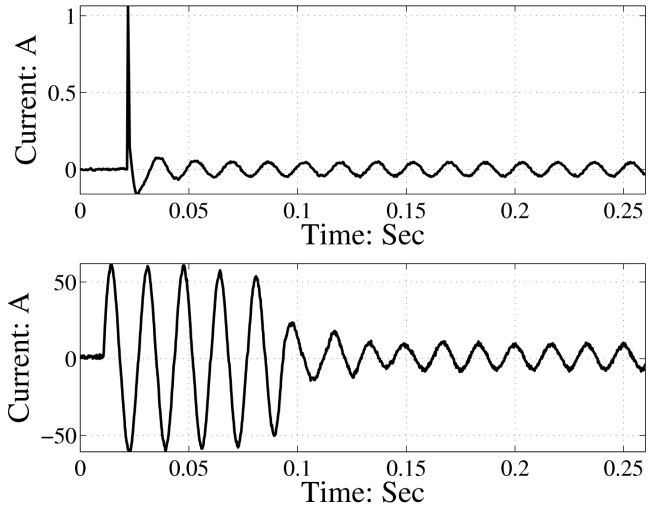

Fig. 3. Top trace: Current drawn during the start of an incandescent lamp. Bottom trace: Stator current drawn during the start of an unloaded, fractional horsepower induction machine.

The final block in Fig. 2 is the NILM's diagnostics and systems management module. This software unit assesses load status using any required combination of current data, voltage data, spectral envelopes, and load operating schedules [11]. The successful application of this module has been demonstrated in numerous publications [1], [2], [3], [4], [5], [13], [16], [18], [19], [20]. Shipboard applications are highlighted in [1], [2], [3], [4], and [5].

As shown in Fig. 2, the modern NILM can interact with human or automated operators in a number of different ways. For instance, the NILM can use its diagnostic information to command certain loads to either commence or cease operations. Additionally, the NILM can provide regular status reports to the Engineering Officer. To assist in future

maintenance operations, the NILM stores all of the relevant data streams (i.e. currents, voltages, operating schedules, etc.) in either a local or remote database [21]. The NILM's vast storage capabilities make it possible for the operator to perform historical data trending. Note that this off-line analysis can be conducted on a remote PC using convenient software packages such as Microsoft Excel [21].

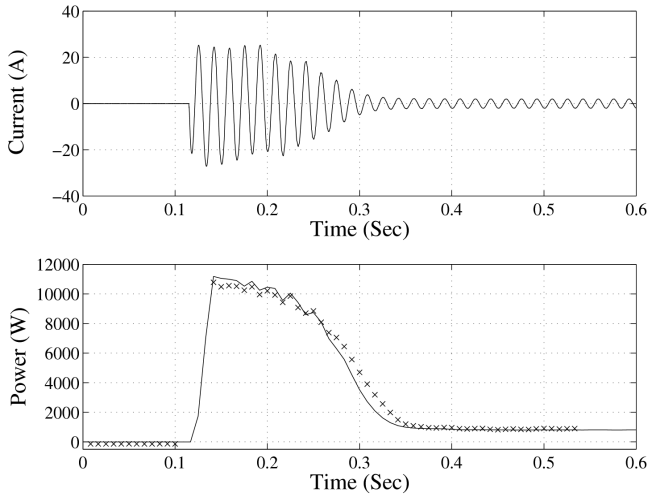

Fig. 4. Measured current and computed power during the start of 1.7hp vacuum pump motor. Also shown in the power plot is a section of the template that has been successfully matched to the observed transient behavior by the NILM's event detector.

IV. Preliminary Field Results at the DDG-51 LBES

To begin testing the NILM's applicability as a shipboard supervisory control system, we have deployed NILM devices throughout the DDG-51 LBES facility for preliminary data collection and assessment. Currently, the following loads and panels are monitored::

- Two Universal Engine Controllers (UECs), one for each GTM
- Shaft Control Unit (SCU)
- #1 Low-Pressure Air Compressor (LPAC)
- 2A Fuel-Oil Service Pump
- 2A Lube-Oil Service Pump
- Full Authority Digital Control (FADC) Local Operating Panel (LOCOP) for control of a single AG9140 GTG
- Distribution panel for GTM controllers and GTM support loads (i.e. igniters, fans, etc.)

The following sections detail the findings obtained during our preliminary tests. To highlight the vast capabilities of the NILM, three different sets of findings are presented – those related strictly to the gas-turbine controllers, those related strictly to electromechanical support loads, and those related to both controllers and support loads.

A. Controller Monitoring

The NILM is ideally suited to monitor the controllers that operate the gas turbines in the DDG-51 engineering plant. These controllers perform several important functions, including control of the electromechanical actuators that admit fuel and starting air into the turbine. Aboard the DDG-51 and other gas-turbine-powered vessels, these controllers consist of small digital computers and power converters that provide either AC or DC power to the appropriate actuators [22], [23]. In general, these devices are non-linear loads that draw harmonically rich line currents. By monitoring these currents, the NILM is able to determine information about the status of valves and other devices. Because one controller powers many other loads, the use of the NILM in this context presents a significant potential reduction in sensor count.

The two sections below describe how the NILM can be used to monitor the controllers for both the GTMs and the GTGs. Several possible analytical tools are also discussed.

1) GTMs: Two different systems are used to control the operation of each GTM aboard the DDG-51. The first of these, which is a Universal Engine Controller (UEC), operates the actuators inside the turbine module. Two key sets of devices under its direct control are the fuel-oil shutoff valves (FOSVs) and the starter-air regulating valve (SARV). These actuators are solenoid valves that receive 28VDC control signals from a power converter inside the UEC. The UEC computer also performs many other monitoring and control functions. For instance, it provides low-level signals that control the application of single-phase AC to the ignition exciters [23].

Each GTM is also affected by the operation of the Shaft Control Unit (SCU). The purpose of this system is to monitor and control any propulsion-related devices that are not under the operation of the UEC. For example, a power converter inside the SCU energizes solenoid valves and other devices outside of the turbine module. The SCU also performs many important computational functions and provides low-level signals to the electronic device that sets the shaft output power [23].

Figure 5 shows typical power data obtained by the NILMs monitoring the SCU and the UEC during a normal start of the 2B turbine. As the turbine progresses through the start procedure, the power drawn by each controller changes, and these changes can be linked to physical events such as valve openings. Starting a turbine requires the actuators to operate in a particular sequence, so the transitions between different power levels should always occur in a prescribed order. For example, when a turbine starts, the UEC first energizes the SARV, which admits compressed air into the starter [23]. As a result the UEC power increases slightly. Once the turbine has reached approximately 1200 rpm, the UEC opens the FOSVs to start the flow of fuel and it orders the igniters to fire [23]. During the start used to generate Fig. 5, this occurred at approximately minute 28.3. As the turbine approaches 4500 rpm, the UEC closes the SARV and commands the ignition circuits to power down [23]. This operation causes the UEC power to drop slightly. In Fig. 5 this transition occurs around minute 28.9. At this point the turbine has reached its self-sustaining speed, and it will remain in operation until the

FOSVs are closed [23]. When that occurs, the UEC power will return to its original pre-start value.

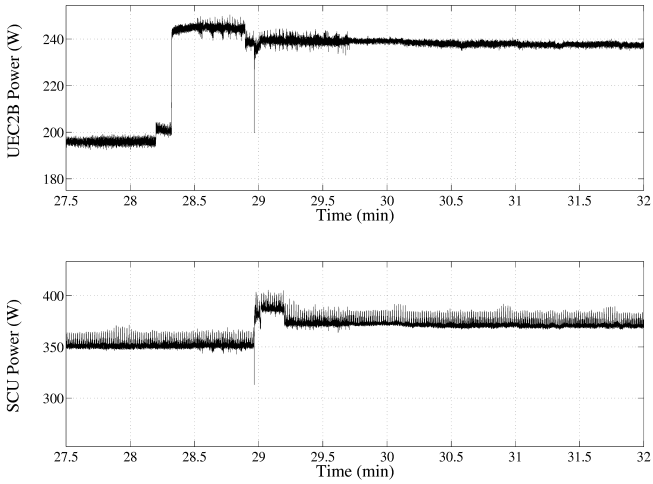

Fig. 5. Power drawn by a UEC and the SCU during a normal turbine start. Note that the start begins around minute 28.2.

One way to enable a NILM to track power transitions is to summarize them using a simple finite-state machine (FSM). Figure 6, for example, is a finite-state diagram that corresponds to the set of actuator operations performed by the UEC during a turbine start. Initially, both the FOSVs and the SARV are closed, so the UEC would be in the top-most state shown in Fig. 6. Once the SARV is opened and the input power increases, the UEC moves to the next state. Similarly, other power transitions trigger other state transitions. When the turbine is powered down, the UEC is returned to its original state. Using FSM models, the NILM can determine if individual actuators are functioning properly and in the appropriate sequence. Methods for tracking finite-state behavior are described in [24].

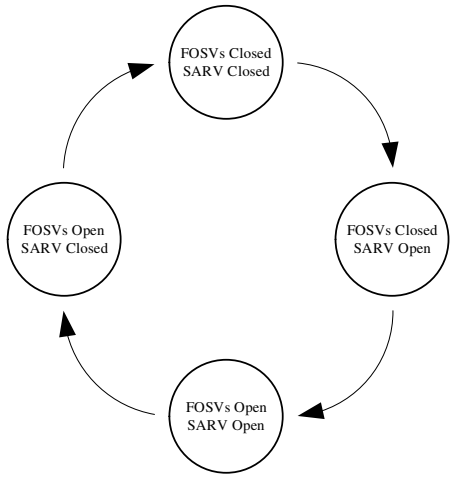

Fig. 5. Finite-state machine model corresponding to the level transitions that occur on the UEC input bus during normal turbine operation. The initial state is the one shown at the top in which both the SARV and FOSVs are closed.

Finite-state machine models can also be used to monitor the operation of the SCU. For instance, Fig. 5 shows that the SCU input power also progresses through a prescribed set of power transitions during a turbine start. Once the turbine has reached its idle speed, the SCU energizes a damper external to the module, forcing the damper to open. At the same time, the SCU also issues a command instructing a large 440VAC cooling fan to turn on [22]. Several minutes after the turbine is brought to a stop, the fan is commanded to de-energize and the dampers are closed. Figure 7 is an FSM model that summarizes the causes of the power transitions on the SCU input bus. Note that this FSM only considers the actions of electromechanical actuators that are directly powered by the SCU; thus, it does not include transitions associated with changes in computational load[1]. More advanced models could take such changes into account.

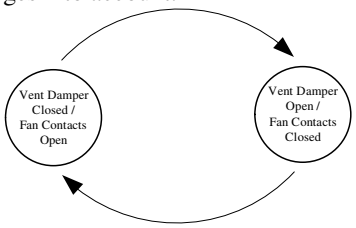

Fig. 7. Finite-state machine model corresponding to the level transitions that occur on the SCU input bus during normal turbine operation. The initial state is the one shown at the left. This FSM considers only electromechanical actuators that are controlled by the SCU.

The finite-state machine approach can be used to track a number of other controller activities. For example, two other common turbine operations are motoring and fuel purging. During a motoring operation, the SARV is opened to allow the turbine to spin using only compressed air. The pressure of the air that enters the module during this procedure is reduced by energizing the motor air regulating valve (MARV) that is in series with the SARV [22]. Figure 8 shows the power drawn by both the SCU and the UEC during this operation. The increase in SCU power corresponds to the action of the MARV; the increase in UEC power corresponds to the action of the SARV. FSM models for both controllers are shown in Fig. 9.

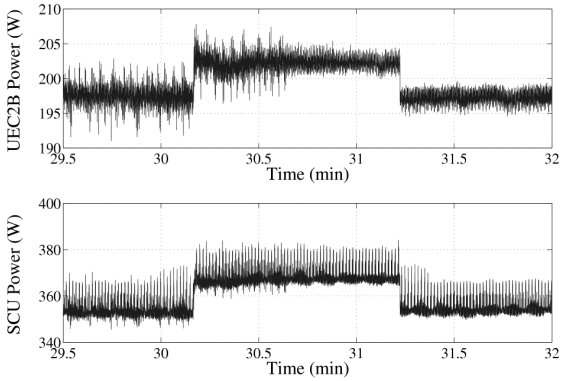

Fig. 8. Power drawn by a UEC and the SCU during a motoring operation. In this case the operator requested a 60s motor.

[1] The short-term change that follows the step change in Fig. 5 is believed to be due to a change in computational load, for instance.

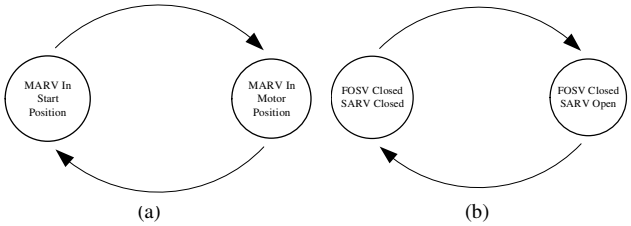

Fig. 9. Finite-state machine models corresponding to motoring operations. a) FSM describing SCU operations and b) FSM describing UEC operations.

Fuel purging causes finite-state behavior similar to that observed during motoring. To purge a turbine of any residual fuel, the controllers must first begin a motoring operation. While the turbine is motoring, the SCU energizes the fuel purge solenoid valve [22]. Figure 10 shows typical input power waveforms for the two controllers, and Figure 11 shows the corresponding FSM diagram for the SCU. Note that the finite-state diagram for the UEC is the same as the one used during motoring.

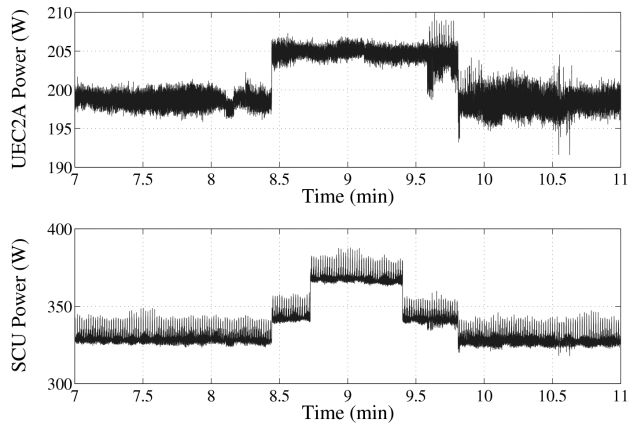

Fig. 10. Power drawn by a UEC and the SCU during a fuel purge operation. In this case the operator requested a 90s purge.

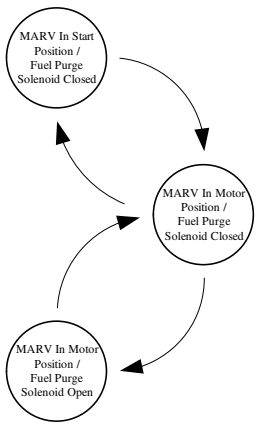

Fig. 11. FSM diagram summarizing the operations performed by the SCU during a fuel purge. The FSM for the UEC is the same as in Fig. 9b.

2) GTGs: The finite-state behavior of the GTG controllers is very similar to that observed for the GTM controllers. Each of the monitored GTGs at the LBES is equipped with a Full Authority Digital Control (FADC) Local Operating Panel (LOCOP). This panel controls both the main gas turbine and its Redundant Independent Mechanical Start System (RIMSS) [7].

The RIMSS consists of a small gas turbine that is mechanically coupled to the GTG. During a GTG start, a small DC motor first spins the RIMSS turbine. Eventually, fuel is admitted into the RIMSS gas-producer turbine and it is ignited. When the gas-producer turbine has reached approximately 40,000 rpm, the RIMSS power turbine begins to rotate and engages the main turbine through a gearbox [7].

In order to allow the GTG to start from "dark" conditions, a No Break Power Supply (NBPS) with a rechargeable battery is used to power the FADC LOCOP. The NBPS is connected to a 440VAC distribution panel and provides 28VDC to the FADC LOCOP. The LOCOP ultimately determines how this power is routed to various relays and solenoids [7]. Currently, a NILM is installed on the AC input bus for the NBPS.

Figure 12 shows the real power drawn by the NBPS during the start of a GTG. Based on information in the technical manual, nine different state changes are expected [25]. Table I lists the devices that either start or stop at each state transition. A close examination of Fig. 12 reveals that each state is discernible. It is important to note, however, that the system progresses rapidly through many of the early states. This expediency is expected, as many of the early transitions affect the operation of the RIMSS, which accelerates at a much higher rate than the primary turbine. The rapid acceleration of the RIMSS is clearly demonstrated by the speed data presented in Fig. 13.

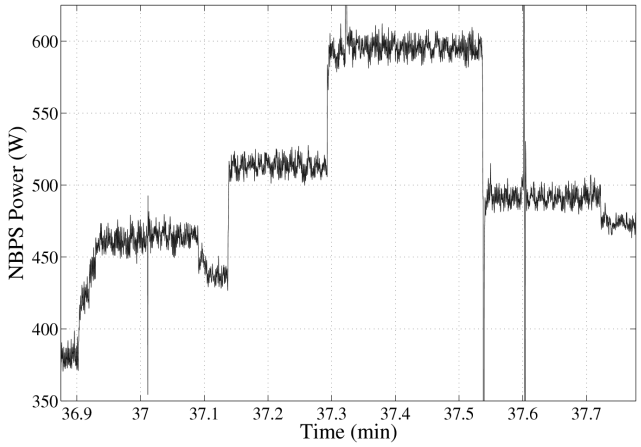

Fig. 12. Power drawn by the NBPS during a GTG start. The transitions correspond to the actions of various relays and solenoids. Note that several of the early transitions occur in rapid succession.

Many other operations performed by the LOCOP manifest themselves in the power drawn by the NBPS. For instance, the bleed air valves on the main turbine are actuated by solenoids on the 28VDC bus [7]. Field results have demonstrated that FSM models can also be created for these events.

TABLE I
STATES IN THE GTG START FSM

State Number	Actions That Trigger Transition Into State
0 (OFF)	N/A
1	1. RIMSS Exhaust Damper Opens 2. GTG Enc. Cooling Unit Dampers Open 3. RIMSS Starter Motor Energized
2	RIMSS Igniter Energized
3	RIMSS Fuel Shutoff Valve Energized (Open)
4	RIMSS Igniter De-energized
5	RIMSS Starter Motor De-energized
6	1. Aux. Lube Oil Pump Started 2. Fuel Manifold Drain Valves Energized (Open)
7	1. K34 Igniters Energized 2. Fuel Manifold Drain Valves De-energized (Closed) 3. Fuel Shutoff Valves Energized (Open) 4. Fuel Paralleling Valve Energized (Parallel Operation)
8	1. K34 Igniters De-Energized (Off) 2. Fuel Paralleling Valve De-Energized (Series Operation)
9	Aux Lube Oil Pump Stopped

B. Electromechanical Support Loads

At the LBES, NILMs also monitor several important electromechanical support loads on the 440VAC bus. Examples include the #1 low-pressure air compressor (LPAC) and the 2A Fuel-Oil Service Pump. An important function of these NILMs is to evaluate the status of the loads. NILM-based diagnostic methods that can be applied to these loads are described in several publications [1], [2], [3], [13], [18].

One intriguing finding that has been made during our work at the LBES is that the NILM can determine the status of certain purely mechanical components. For example, Fig. 14 shows the power drawn by a low-pressure air compressor before, during, and after the air start of a gas-turbine generator. During and after the start, low-pressure air is needed to actuate several valves. As a result, air demand increases, causing the compressor to load for a longer time period and to remain unloaded for a shorter time period. Fig. 15 shows how the start affects the lengths of the load and unload intervals. By searching for such characteristic patterns, the NILM can identify the operation of the appropriate pneumatic valves. This capability can be used to detect critical faults such as valve failures and leaks. This ability is discussed further in the next section.

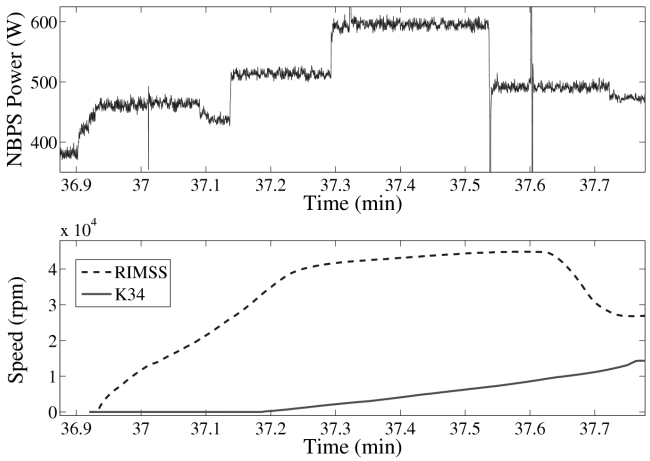

Fig. 13. NBPS input power and turbine speeds during a GTG start. The trace labeled "RIMSS" is the speed of the RIMSS gas-producer turbine, and the trace labeled "K34" is the speed of the primary turbine. Note that the RIMSS turbine accelerates rapidly during the early states.

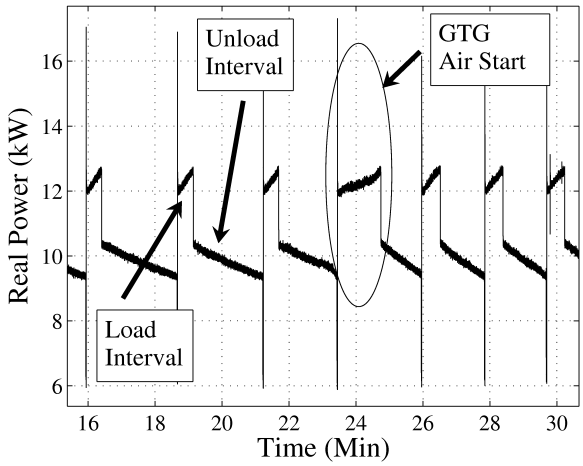

Fig. 14. Power consumption by the #1 LPAC before, during, and after the air start of one of the GTGs.

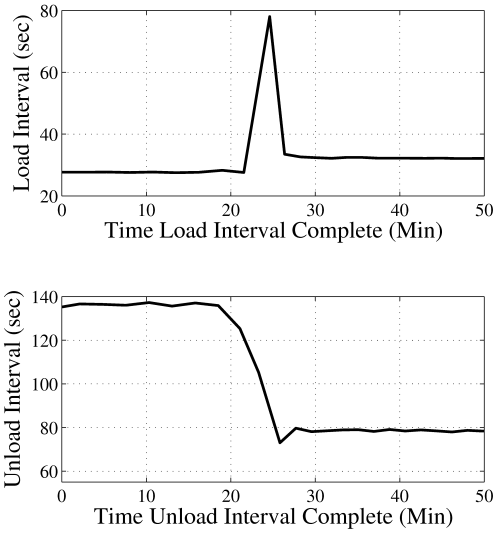

Fig. 15. Time histories showing variations in the lengths of the LPAC's load and unload intervals. These time histories were created using the data shown in Fig. 14.

C. Monitoring Multiple Loads

By monitoring the power flowing to multiple loads, many new diagnostic features can be implemented. One example is the detection of leaks in the compressed-air system. To detect such faults, the NILM can try to correlate controller actions with long-term trends in the load on the compressor. As a specific example, consider Fig. 16, which shows the evolution of the load and unload intervals over a nearly seven-hour window. During that period, the load on the compressor experienced three long-term shifts. As indicated in the figure, two of those three changes were the result of controller-issued commands. The third shift, however, occurred because a small leak was inserted into the system using a flow meter. With no accompanying controller command, the NILM would consider this change to be a leak. Multi-scale techniques are currently being investigated for use in detecting leaks that build slowly over time.

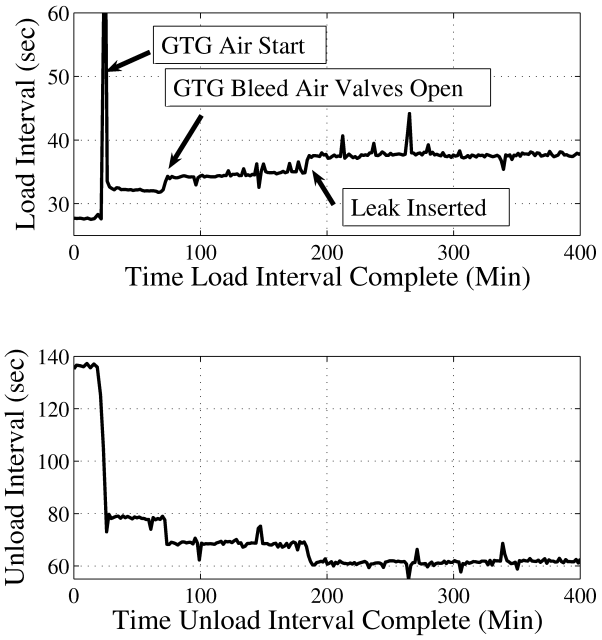

Fig. 16. Time histories showing variation in the LPAC's load and unload intervals over a nearly seven-hour window. The top trace is annotated to indicate the physical event that caused the three long-term shifts. .

V. Ongoing and Future Work

To further the development of a NILM-based supervisory control system, several new projects are currently underway. First, we are expanding our software suite so that the NILM can log several critical electrical parameters. Example quantities include the following:

- Generator load
- Line frequency
- Voltage amplitude
- Harmonic distortion

By logging these features, a NILM placed on the generator output bus could potentially perform many of the monitoring and control functions that are now performed by the LOCOP[2]. The benefit of this approach would be that the NILM could simultaneously evaluate the status of loads downstream from the generator.

Another ongoing project is the development of a system that minimizes the overall level of intrusion. As a preliminary step, we have installed a NILM on the distribution panel that feeds all of the GTM controllers and several critical support loads. The monitored loads include the following:

- UEC2A
- UEC2B
- SCU
- Igniters for the 2A GTM
- Igniters for the 2B GTM
- Lighting and heating for the various turbine modules and controllers

Figure 17 shows some results from our initial tests. The data presented in that figure was recorded during a GTM start. Note that the level transitions in each of the component streams are still visible in the aggregate. Furthermore, note that we are now able to monitor the behavior of the igniters. It is worth noting that the igniters inside the 2A turbine draw power waveforms that display a significant amount of high frequency content. This is not the case for the 2B turbine, suggesting that there may be opportunities to develop new and critical diagnostic indicators.

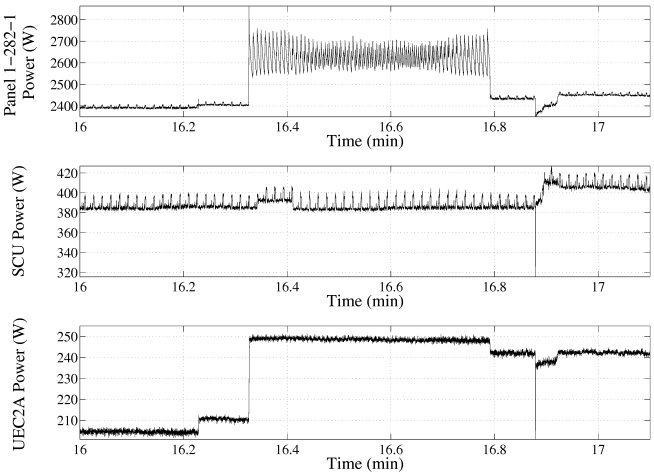

Fig. 17. Power drawn during start of the 2A GTM. The top trace is the aggregate power drawn by distribution panel 1-282-1. The large, noisy change in the aggregate stream is the result of the igniters. Note that the level transitions in each of the component streams are visible in the aggregate. The small disturbance located at approximately minute 16.9 is the result of a sub-transient voltage sag. The source of this is sag is believed to be the large fan that cools the turbine. This sag is visible throughout the plant.

Figure 17 highlights another potential benefit of the NILM. Note the disturbance located in each of the data streams at approximately minute 16.9. This disturbance is the result of a

[2] It is important to note that the NILM already has the ability to measure the key electrical quantities described here. The features that need to be incorporated into the NILM are the real-time control activities that rely on this information.

sub-transient voltage sag. Field tests have shown that this sag, which is visible throughout the plant, occurs at the same time that the SCU commands the large cooling fan to energize. The ability to identify the source and effects of such power-quality disturbances could make the NILM indispensable to the all-electric warships of the future.

Although we have already had success in placing the NILM upstream of its monitored loads, we continue to press for an even less intrusive alternative. Currently, we are developing instrumentation and software that can be used to better detect the small power changes that are caused by the operation of small loads such as solenoids and relays. We expect to begin field tests within the next six months.

VI. Acknowledgment

The authors gratefully acknowledge the assistance and support provided by the crew at the DDG-51 LBES. In particular, we thank Andy Cairns, Charlie Gilligan, and Lee Skarbeck. We also thank the LBES crew for providing the speed data presented in Figure 13.

VII. References

[1] R. W. Cox, J. P. Mosman, D. McKay, S. B. Leeb, and T. J. McCoy, "Diagnostic indicators for shipboard cycling systems using non-intrusive load monitoring," in *Proc. ASNE Day 2006*, Arlington, VA.

[2] T. DeNucci, R. W. Cox, S. B. Leeb, J. Paris, T. J. McCoy, C.R. Laughman, and W. C. Greene, "Diagnostic indicators for shipboard systems using non-intrusive load monitoring," in *Proc. 1st IEEE Electric Ship Technologies Symposium*. Philadelphia, PA.

[3] R. W. Cox, G. Mitchell, J. Paris, and S. B. Leeb, "Shipboard fluid system diagnostic indicators using non-intrusive load monitoring," to appear in *Proc. ASNE Day 2007*, Arlington VA.

[4] R. W. Cox, G. Mitchell, P. Bennett, M. Piber, J. Paris, W. Wichakool, and S. B. Leeb, "Improving shipboard maintenance practices using non-intrusive load monitoring," to appear in *Proc. ASNE Intelligent Ships VII* , Philadelphia, PA.

[5] J. S. Ramsey, S. B. Leeb, T. DeNucci, J. Paris, M. Obar, R. W. Cox, C. R. Laughman, and T. J. McCoy, "Shipboard applications of non-intrusive load monitoring," in *Proc. ASNE Reconfiguration and Survivability Symposium,* Atlantic Beach, FL, 15-18 Feb. 2005.

[6] T. D. McKay, "Diagnostic indicators for shipboard mechanical systems using non-intrusive load monitoring," S.M./N.E. Thesis, Mech. Eng., MIT, 2006.

[7] H. J. Kozuhowski, M. G. Hoffman, C. D. Mako, L. L. Overton, and W. E. Masincup, "Integrated testing of the full authority digital control and redundant independent mechanical start system for the U.S. Navy's DDG-51 ship service gas turbine generator sets," in *Proc. ASME TURBO EXPO*, Stockholm, 1998.

[8] M. DiUlio, C. Savage, and E. Schneider, "Taking the integrated condition assessment system to the year 2010," in *Proc. 13th International Ship Control Systems Symposium*, Orlando, FL, Apr. 2003.

[9] R. J. Bost, J. G. Mellis, and P. A. Dent, "Is the Navy serious about reducing manning on its ships?" Office of Naval Research, 1999.

[10] R. L. Lopushansky, "All optical shipboard sensing system," in *Proc. 45th International Instrumentation Symposium,* Albuquerque, NM, May 1999.

[11] R. W. Cox, "Minimally intrusive strategies for fault detection and energy monitoring," Ph.D. dissertation, EECS, MIT, Aug 2006.

[12] S. B. Leeb, S. R. Shaw, and J. L. Kirtley, "Transient event detection in spectral envelope estimates for nonintrusive load monitoring," *IEEE Trans. on Power Delivery*, vol. 10, no. 3, pp. 1200–1210, July 1995.

[13] S. R. Shaw, "System identification techniques and modeling for non-intrusive load diagnostics," Ph.D. dissertation, EECS, MIT, Feb. 2000.

[14] S. R. Shaw, C. B. Abler, R. F. Lepard, D. Luo, S. B. Leeb, and L. K. Norford, "Instrumentation for high performance nonintrusive electrical load monitoring," *ASME Journal of Solar Energy Engineering*, vol. 120, pp. 224-229, Aug 1998.

[15] A. V. Oppenheim, A. S. Willsky, and I. T. Young, Signals and Systems. Prentice Hall Signal Processing Series, Englewood Cliffs, New Jersey: Addison Wellesley, 1988.

[16] K. D. Lee, "Electric load information system based on non-intrusive power monitoring," Ph.D. dissertation, Mech.. Eng, MIT, May 2003.

[17] S. B. Leeb, "A conjoint pattern recognition approach to nonintrusive load monitoring," Ph.D. dissertation, EECS, MIT, Feb. 1993.

[18] P. R. Armstrong, C. R. Laughman, S. B. Leeb, and L. K. Norford, "Detection of rooftop cooling unit faults based on electrical measurements," HVAC+R Research Journal, vol. 12, no. 1, pp. 151–175, Jan. 2006.

[19] D. Luo, "Detection and diagnosis of faults and energy monitoring of HVAC systems with least- intrusive power analysis," Ph.D. dissertation, Dept. Arch., MIT, Feb. 2001.

[20] C. R. Laughman, P. R. Armstrong, L. K. Norford, and S. B. Leeb, "The detection of liquid slugging phenomena in reciprocating compressors via power measurements," in *Proc. International Compressor Engineering Conference at Purdue*, pp 1-8, West Lafayette, IN, Jul 2006.

[21] J. Paris, "A framework for non-intrusive load monitoring and diagnostics," M.Eng. Thesis, EECS, MIT, Feb. 2006.

[22] *Technical Manual for LM2500 Propulsion Gas Turbine*, Naval Sea Systems Command, S9234-AD-MMO-010/LM2500, 26 May 2000.

[23] *Technical Manual for Universal Engine Controller*, Naval Sea Systems Command, S6263-B7-MMA-010, 25 Nov 2002.

[24] G. W. Hart, "Nonintrusive appliance load monitoring," *Proc. of the IEEE*, vol. 80, no. 12, pp. 1870-1890, Dec 1992.

[25] *Technical Manual for AG9140RF Ship Service Gas Turbine Generator (SSGTG)*, Naval Sea Systems Command, S9311-XX-MMO-010, Mar 2003.